Virology 612 (2025) 110694

Contents lists available at ScienceDirect

Virology

journal homepage: www.elsevier.com/locate/virology

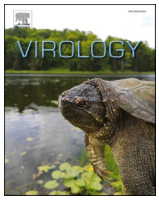

Brief Communication

The VP7 protein of the African horse sickness virus core particle facilitates binding to *Culicoides sonorensis* cells in an RGD-independent manner

Ariel Renée Monique Buyens, Vida van Staden, Jacques Theron *

Department of Biochemistry, Genetics and Microbiology, University of Pretoria, Pretoria, 0002, South Africa

ARTICLE INFO

Keywords:
African horse sickness virus
VP7
RGD motif
Cell binding

ABSTRACT

African horse sickness, caused by African horse sickness virus (AHSV) that is transmitted by midges of the *Culicoides* genus, leads to rapid mortality among horses. Proteases in the saliva of *Culicoides* midges cleave the VP2 outer capsid protein, resulting in infectious sub-virus particles that have increased infectivity for the *Culicoides* vector insect and *Culicoides*-derived cells (KC cells). The AHSV VP7 protein has an arginine-glycine-aspartate (RGD) motif, but the functional relevance of this protein and motif in facilitating binding to insect cells is unknown. To investigate, core-like particles (CLPs) were produced using the baculovirus expression system through the co-expression of VP3 and sVP7, which is a soluble version of the AHSV-4 VP7 protein. Insect cell binding assays indicated that the CLPs bind to KC cells, suggesting a role for VP7 in this interaction. Subsequently, recombinant baculoviruses expressing mutant sVP7 proteins were synthesized, in which the RGD motif was either deleted or mutated. All RGD-mutated sVP7 proteins, except for the deletion of the RGD motif, formed trimers and, when co-expressed with VP3, assembled into CLPs that retained the ability to bind to insect cells. These findings indicate that VP7 facilitates the binding of CLPs to insect cells through an RGD-independent mechanism.

1. Introduction

African horse sickness (AHS), of which African horse sickness virus (AHSV) is the causative agent, is a highly lethal disease affecting horses. Mortality rates can reach up to 95 % in naïve horse populations (Mellor and Hamblin, 2004), and consequently, AHS is classified as a notifiable equine disease by the World Organization for Animal Health (WOAH). The disease is endemic in sub-Saharan Africa, with occasional outbreaks in North Africa, Asia, and southern Europe (Zientara et al., 2015; King et al., 2020).

AHSV, a member of the *Orbivirus* genus within the family *Sedoreoviridae*, exhibits a double icosahedral capsid. The outer capsid layer comprises the two major structural proteins VP2 and VP5, whereas the innermost capsid is composed of the VP3 and VP7 proteins (Manole et al., 2012). The core particle contains a genome of ten linear segments of double-stranded RNA and the three minor proteins VP1, VP4 and VP6, each of which plays an important role in genome RNA replication (Patel and Roy, 2014).

AHSV is primarily transmitted through the bites of midges from the genus *Culicoides* (Carpenter et al., 2017). Proteases (trypsin and chympotrypsin) present in the saliva of *Culicoides* midges cleave the VP2 outer capsid protein, resulting in infectious sub-virus particles that have increased infectivity for the *Culicoides* vector insect and *Culicoides*-derived cell lines (Darpel et al., 2011; Marchi et al., 1995; Mertens et al., 1996). This indicates that infectious sub-virus particles, whether with a non-modified or modified outer capsid protein VP5, are infectious for the insect vector. As the five-fold axis of the core particle is exposed on the surface of the infectious virus particle (Manole et al., 2012), it was subsequently reported that an arginine-glycine-aspartate (RGD) tripeptide sequence present on the outermost core protein VP7 of bluetongue virus (BTV), the prototype orbivirus species, is responsible for *Culicoides* cell binding activity (Xu et al., 1997; Tan et al., 2001). The AHSV VP7 protein also contains an RGD motif (Basak et al., 1996), but the functional relevance of this protein and motif in facilitating binding to insect cells is not yet known.

The AHSV VP7 protein is insoluble and has the unique property of forming flat hexagonal crystals of varying size in the cytoplasm of virus-infected cells (Burroughs et al., 1994; Bekker et al., 2014). The functional significance of the VP7 crystalline structures is not yet understood, although it has been suggested that the propensity of VP7 to form

* Corresponding author.
E-mail addresses: buyensariel@gmail.com (A.R.M. Buyens), vida.vanstaden@up.ac.za (V. van Staden), jacques.theron@up.ac.za (J. Theron).

https://doi.org/10.1016/j.virol.2025.110694
Received 25 June 2025; Received in revised form 12 September 2025; Accepted 15 September 2025
Available online 15 September 2025

crystalline particles may sequester the available soluble VP7 trimers and thus negatively impact the assembly of AHSV cores (Maree et al., 2016). Research on AHSV VP7 has focused on the self-assembly of the crystalline particles, aiming to elucidate the mechanism by which they are formed (Bekker et al., 2014, 2017), and culminated in the availability of a soluble version of the AHSV VP7 protein (sVP7) that does not form crystalline particles but retained the ability to interact with VP3 to form core-like particles (CLPs) (Bekker et al., 2022a, 2022b). The availability of a soluble version of the VP7 protein has opened the door to new research opportunities relating to the structure-function relationships of the AHSV VP7 protein.

In this study, we investigated the functional importance of the RGD motif on VP7 of AHSV for attachment to *Culicoides sonorensis*-derived (KC cells). To this end, wild-type and RGD-mutated CLPs composed of VP3 and sVP7 were produced using the baculovirus expression system, purified and then evaluated for their ability to bind to KC cells with an ELISA-based cell binding assay. Our results indicate that the AHSV VP7 protein binds to insect cells but that the binding activity occurs independently of the RGD motif.

2. Materials and methods

2.1. Cell culture

Spodoptera frugiperda clone 9 (Sf9) cells were maintained as adherent cultures in cell culture flasks (Sigma-Aldrich) in TC-100 medium (Gibco) supplemented with 10 % (v/v) foetal bovine serum (FBS; Gibco) and antibiotics (2.26 μg/ml amphotericin B, 100 μg/ml penicillin, 100 μg/ml streptomycin; Lonza). Suspension cultures of Sf9 cells in 250-ml Erlenmeyer flasks (150 rpm) were maintained in the same medium, with the addition of 1 % (v/v) Pluronic-F68 (Sigma-Aldrich). Cell monolayers and suspension cultures were incubated at 28 °C.

2.2. Construction of recombinant pFastBac 1 donor plasmids

The AHSV-4 VP3 gene and a mutated version of the AHSV-4 VP7 gene, designated VP7-276, that encodes a soluble VP7 (sVP7) protein (Bekker et al., 2022a), were each cloned into a pFastBac 1 donor plasmid (Thermo Fisher Scientific). For this purpose, the VP3 gene was digested with *Xho*I and *Kpn*I (New England Biolabs) and cloned into the *Xho*I and *Kpn*I sites of the plasmid, thereby generating VP3 pFB. The sVP7 gene was digested with *Bgl*II and *Eco*RI (Thermo Fisher Scientific) and cloned into the *Eco*RI and *Bam*HI sites of the plasmid, thereby generating sVP7 pFB. The cloned insert DNA was characterized by nucleotide sequencing with the ABI-PRISM BigDye Terminator v.3.1 Cycle Sequencing Ready Reaction kit (PerkinElmer Applied Biosystems), followed by resolution of the extension products on an ABI-PRISM 3130XL DNA sequencer.

For construction of sVP7 genes in which the RGD motif (nucleotide positions 532–540) was either deleted or contained site-specific mutations, an inverse PCR-based method of mutagenesis was used. Plasmid sVP7 pFB was used as template together with appropriately designed back-to-back mutagenic primers (Table 1). Inverse PCR reactions were performed using Phusion Hot Start DNA polymerase (Thermo Fisher Scientific) in a BioRad T100 thermal cycler. The thermal cycling parameters consisted of initial denaturation at 98 °C for 30 s, followed by 25 cycles of denaturation at 98 °C for 10 s and annealing and extension at 72 °C for 90 s. Non-mutant plasmid DNA template was removed by incubation with 10 U of *Dpn*I (Thermo Fisher Scientific) at 37 °C for 15 min. The amplicons were purified, phosphorylated in the presence of 10 U of T4 Polynucleotide kinase (New England Biolabs) and then self-ligated at 22 °C for 1 h in the presence of 5 U of T4 DNA ligase (Thermo Fisher Scientific). The derived plasmid DNA constructs were subjected to DNA sequencing, as described above, to confirm the presence of the newly introduced mutations.

Table 1
Mutagenic primers used for mutagenesis of the RGD motif in the sVP7 gene.

Mutation	Primer	Sequence (5' - 3')
AGD	iPCR-AF	AGCCCCAAGGGCGGGGGACGCAGTCATG
	iPCR-AR	AGCAGCGCATTGACCTGTCCCGCAGCGCC
KGE	iPCR-KF	TAGCCCCAAGGAAAGGGGAAGCAGTCATGATC
	iPCR-KR	GCAGCGCATTGACCTGTCCCGCAGC
HLE	iPCR-HF	CTAGAAGCAGTCATGATCTATTTTGTTTGGAGACC
	iPCR-HR	GTGCCTTGGGGCTAGCAGCGCATTGACC
Deletion	iPCR-DF	GCAGTCATGATCTATTTTGTTTGGAGACCA
	iPCR-DR	CCTTGGGGCTAGCAGCGCATTGAC

Grey shading indicates mutations in the primer sequences.

2.3. Generation of recombinant baculoviruses

Recombinant baculoviruses were generated with the Bac-to-Bac baculovirus expression system (Thermo Fisher Scientific). Briefly, the recombinant bacmid donor plasmids were transformed into competent *E. coli* DH10Bac cells, and recombinant bacmids were selected by plating the transformed cells onto LB agar supplemented with 50 μg/ml of kanamycin, 7 μg/ml of gentamycin and 10 μg/ml of tetracycline in the presence of 50 μl of 2 % (w/v) X-gal and 10 μl of 100 mM IPTG. The agar plates were incubated at 37 °C for 48 h and transformants displaying a white-colony phenotype were selected. Bacmid DNA was subsequently extracted and then transfected into Sf9 cells with Cellfectin II Reagent (Gibco) according to the manufacturer's instructions. Following incubation at 28 °C for 96 h, the medium was collected, centrifuged at 1000×*g* for 5 min and the cell-free supernatants, containing the recombinant baculovirus, were passaged twice of Sf9 cells for virus amplification.

2.4. Immunoblot analysis

Recombinant protein expression, and the preparation and fractionation of cell lysates were performed according to the procedures described by French and Roy (1990). The Sf9 cells were infected at a multiplicity of infection (MOI) of 5 plaque forming units (pfu)/cell, and were incubated at 28 °C for 48 h. The cells were harvested by centrifugation at 500×*g* for 5 min, washed with 1 × phosphate-buffered saline (PBS), suspended in TNN lysis buffer (50 mM Tris, 150 mM NaCl, 0.5 % [v/v] Nonidet P-40; pH 8) and lysed at 4 °C. The cell lysate was centrifuged at 500×*g* for 5 min and the supernatant was recovered as the cytoplasmic protein fraction. Protein samples were mixed with 2 × Laemmli buffer (65.8 mM Tris [pH 6.8], 2.1 % [w/v] SDS, 5.27 % [v/v] β-Mercaptoethanol, 26.3 % [v/v] Glycerol, 0.01 % [w/v] Bromophenol blue) and incubated at 100 °C for 5 min. Alternatively, for the detection of VP7 trimers, the protein samples were mixed with Protein dissociation buffer (10 % [v/v] β-Mercaptoethanol, 10 % [w/v] SDS, 25 % [v/v] Glycerol, 10 mM Tris [pH 6.8], 0.02 % [w/v] Bromophenol blue) and incubated at 40 °C for 10 min (Monastyrskaya et al., 1997).

The recombinant baculovirus-expressed proteins were resolved by electrophoresis in a 10 % SDS-PAGE, as described by Laemmli (1970). For immunoblot analysis, proteins from an unstained SDS-polyacrylamide gel were electroblotted onto a Hybond-C^{+} Extra nitrocellulose membrane (Amersham Pharmacia Biotech), as described by Blancher and Jones (2001). The membrane was incubated for 30 min at room temperature in blocking solution (1 % [w/v] fat-free milk powder in 1 × PBS), followed by incubation with a polyclonal anti-VP3 or/and anti-VP7 antibody (GenScript Corp.) that were each diluted 1:2000 in blocking solution. The blot was washed three times with wash buffer (0.05 % [v/v] Tween-20, 1 × PBS; pH 7.4) and incubated for 2 h at room temperature with the secondary antibody, Protein-A conjugated to horseradish peroxidase (diluted 1:10 000; Sigma-Aldrich). After three successive washes with wash buffer, the blots were rinsed with 1 × PBS and immunoreactive proteins were detected with enzyme substrate solution (200 μl of 3 % [v/v] hydrogen peroxide and 2 ml of 4-chloronapthol [3 mg/ml] in 20 ml of 1 × PBS).

2.5. Synthesis and purification of core-like particles (CLPs)

CLPs were synthesized by co-infection of Sf9 cells with the recombinant baculoviruses expressing either the sVP7 or mutant sVP7 proteins and the recombinant baculovirus expressing VP3, each at a MOI of 5 pfu/cell. The flasks were incubated at 28 °C for 72 h, after which the cells were harvested by centrifugation at 3000×*g* for 5 min at 4 °C, rinsed with 1 × PBS and then suspended in 1 ml TNN buffer. Following incubation on ice for 30 min with agitation at 180 rpm, the cells were homogenized with a pre-chilled Douncer and centrifuged at 500×*g* for 5 min at 4 °C. The clarified supernatant (1 ml) was loaded on a 40–66 % discontinuous sucrose gradient that comprised of 1 ml of 66 % (w/v) sucrose and 3 ml of 40 % (w/v) sucrose prepared in TN buffer (200 mM Tris-HCl [pH 8], 150 mM NaCl) and subjected to ultracentrifugation at 121 570×*g* for 3 h at 4 °C in a SW 55 Ti rotor using an Optima L-80 XP Ultracentrifuge (Beckman Coulter). Fractions of 500 μl were collected from the bottom of the gradient. The fractions containing CLPs were pooled and diluted in 4 ml of TN buffer (200 mM Tris-HCl [pH 8], 150 mM NaCl), followed by ultracentrifugation at 18 000×*g* for 90 min at 4 °C. The CLPs were each suspended in Protein binding buffer (1 × PBS [pH 7.4], 1 mM $MgCl_2$, 1 mM $CaCl_2$), and the concentration of the CLPs was determined with the NanoDrop 2000 Spectrophotometer (NanoDrop Technologies, Inc.).

2.6. Transmission Electron Microscopy (TEM) of CLPs

Sucrose gradient-purified CLPs were adsorbed for 1 min onto Carbon-filmed copper 400-mesh grids. The grids were washed three times by floating the grid on top of 25 μl of ddH_2O for 1 min each time. The CLPs were negatively stained with 2 % (w/v) uranyl acetate by floating the grid on top of 25 μl of the stain for 30 s. Before viewing, the grids were air-dried for 3 min. An immuno-decorating technique described by Gulati et al. (2019) was used to confirm the identity of the CLPs. Grids with purified CLPs were floated on top of 25 μl of a polyclonal anti-VP7 antibody (diluted 1:200 in 1 × PBS), followed by incubation at 4 °C for 1 h. The grids were then washed with ddH_2O and stained with 2 % (w/v) uranyl acetate, as described above. All grids were examined in a Joel 2100F FEG TEM at 100 kV.

2.7. ELISA assay for detection of CLP binding to KC cells

An ELISA-based cell binding assay previously developed for BTV (Tan et al., 2001) was used to evaluate the binding of AHSV CLPs to KC cells. Briefly, sucrose gradient-purified CLPs were diluted in Protein binding buffer and used at concentrations of 0, 6, 12.5, 25, 50, and 100 μg/well. The diluted CLPs were added to the wells of a 96-well tissue culture plate seeded with KC cells and were incubated at room temperature for 30 min. The cells were washed with 1 × PBS, fixed with Fixing buffer (10 % [v/v] 1 × PBS [pH 7.4], 90 % [v/v] ethanol), blocked with Blocking buffer (1 × PBS [pH 7.4], 3 % [w/v] bovine serum albumin [BSA]) and probed sequentially with a polyclonal anti-VP7 antibody (diluted 1:2500 in 3 % [w/v] BSA) and horseradish peroxidase-conjugated Protein-A (diluted 1:2500 in 3 % [w/v] BSA). Binding was detected with Tetramethylbenzidine substrate, and the absorbance at 450 nm was measured with a Multiskan SkyHigh Microplate spectrophotometer (Thermo Fisher Scientific). The cell binding assay was repeated three independent times, with three technical replicates each, and the data is presented as the means ± Standard Deviation (SD). Statistical analyses (one-way ANOVA) were performed in Excel (Microsoft Corp., USA) on the absorbance readings to establish significant binding ($p < 0.05$).

3. Results

3.1. Generation of RGD mutant sVP7 recombinant proteins

To investigate a role for the RGD motif on AHSV VP7 in insect cell binding, recombinant baculoviruses were generated expressing mutant sVP7 proteins, in which the RGD motif was either deleted or mutated by substituting amino acid residues within the RGD motif to AGD, HLE, and KGE. The KGE mutation maintains the positive-neutral-negative charge of the RGD motif. The AGD and HLE mutations imparted a neutral-neutral-negative charge and positive-positive-negative charge, respectively, and were not expected to support binding to integrin receptors on the insect cell surface (Tan et al., 2001). The desired mutated genes were generated using inverse PCR, followed by nucleotide sequencing that confirmed the introduced mutations (Supplementary Fig. 1) and verified the absence of any nucleotide differences aside from the newly introduced site-specific mutations.

To confirm protein expression of the AHSV-4 sVP7 and mutant sVP7 proteins, recombinant baculoviruses were used to infect Sf9 cells and after 3 days post-infection (dpi), the cytoplasmic proteins were subjected to immunoblot analysis. The sVP7 and mutant sVP7 proteins with a molecular mass of 38 kDa were detected, confirming expression (Fig. 1A). Next, the ability of the mutant sVP7 proteins to form trimers, which are essential for core particle assembly (Limn et al., 2000; Manole et al., 2012), was assessed. The cytoplasmic proteins were incubated at 40 °C in the presence of SDS and β-mercaptoethanol, and subjected to immunoblot analysis that revealed that the RGD substitution mutant sVP7 proteins (sVP7-AGD, sVP7-HLE, and sVP7-KGE) formed trimers with a molecular mass of 120 kDa (Fig. 1B). This indicates that these substitution mutations did not impede monomer-monomer interactions and, therefore, these mutant proteins retained the ability to form trimers. In contrast, the mutant sVP7 protein in which the RGD motif was deleted (sVP7-Deletion) was detected solely as a 38 kDa monomer, suggesting that deletion of the RGD motif affected protein folding or conformation, preventing trimer formation. Consequently, the mutant sVP7-Deletion protein was excluded from further investigations.

3.2. Characterization of the RGD-mutant core-like particles (CLPs)

The ability of the RGD-mutant sVP7 proteins to assemble into CLPs when co-expressed with the VP3 protein was evaluated. The expression of the AHSV-4 VP3 protein, required as a scaffold for sVP7 assembly during CLP formation (Bekker et al., 2022a), was first confirmed, as described in section 3.2. Immunoblot analysis detected the VP3 protein with a molecular mass of 103 kDa (Fig. 1A). Subsequently, Sf9 cells were co-infected with a recombinant baculovirus expressing VP3 and another recombinant baculovirus expressing either the sVP7 protein or one of the mutant sVP7 proteins. After 3 dpi, the CLPs were purified by ultracentrifugation through a 40–66 % (w/v) discontinuous sucrose density gradient (Supplementary Fig. 2) and analysed by transmission electron microscopy. The purified RGD-mutated CLPs formed from sVP7-AGD, sVP7-HLE, and sVP7-KGE were similar in size (70 nm) and morphology to the CLPs formed by the sVP7 protein, displaying the characteristic darkly stained central region, surrounded by a less electron-dense outer layer with knobby protrusions radiating outward (Fig. 2A). This aligns with the distinctive ring-like arrangement of VP7 capsomers present on the surface of AHSV CLPs (Bekker et al., 2022a; Maree et al., 2016). The identity of the RGD-mutant CLPs was further confirmed by antibody decoration using an AHSV-4 VP7-specific antibody, which masked the CLPs with a dark shadow in electron micrographs, identical to the sVP7 CLP (Fig. 2B). This indicates that the anti-VP7 antibody interacted with the mutant sVP7 proteins present on the outer surface of the CLPs. These findings suggest that the mutations in the RGD motif of sVP7 did not disrupt the interaction between sVP7 and VP3, nor its ability to form CLPs.

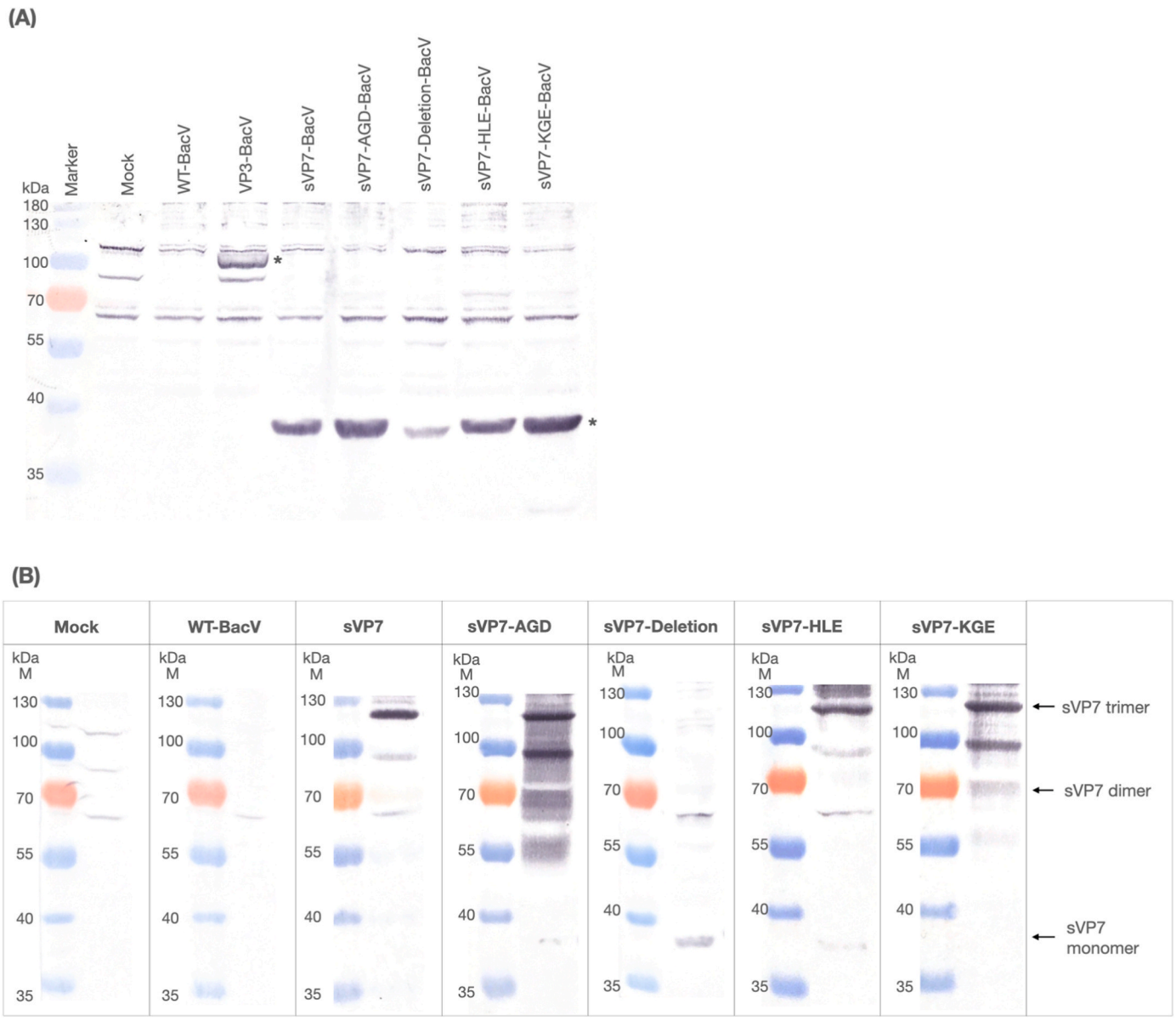

Fig. 1. Immunoblot analysis of recombinant AHSV proteins. Cytoplasmic protein fractions prepared from Sf9 cells infected with recombinant baculoviruses were electroblotted onto a nitrocellulose membrane from unstained SDS-PAGE gels and subjected to immunoblot analysis with a mixture of anti-VP3 and anti-VP7 antibodies (A). The VP3 and the sVP7 and mutant sVP7 proteins are indicated with a black asterisk (A). Cytoplasmic proteins of partially denatured sVP7 and mutant sVP7 proteins at 40 °C in the presence of reducing agents (B). The sVP7 trimer, dimer and monomer positions are indicated to the right of the figures. Cytoplasmic protein fractions prepared from mock-infected Sf9 cells (Mock) and wild-type baculovirus (WT-BacV)-infected cells were included as controls (A, B). The sizes of the protein molecular mass markers are indicated in kDa to the left of the figures.

3.3. AHSV CLPs bind to KC cells in an RGD-independent manner

To assess whether the RGD motif plays a role in the binding of AHSV CLPs to *Culicoides sonorensis* (KC) insect cells, KC cell monolayers were incubated with different concentrations (0–100 μg/well) of sucrose gradient-purified CLPs and the binding of the CLPs was assessed following incubation by an ELISA using an anti-VP7 polyclonal antibody. The results indicated that the sVP7 CLP bound to the KC cells in a concentration-dependent manner (Fig. 2C). Likewise, CLPs generated with the sVP7 mutant proteins containing mutations in the RGD motif all showed a similar level of binding to the KC cells and mirrored the dose-response curve of the sVP7 CLP (Fig. 2C). There was no statistically significant difference ($p > 0.05$) between the binding of the respective CLPs to the KC cells at each of the concentrations used in the assay. These results indicated that the RGD motif present in the sVP7 protein of AHSV-4 does not play a role in the binding of CLPs to insect cells.

4. Discussion

AHSV, a lethal arbovirus affecting equids, is transmitted by *Culicoides* midges (Mellor and Hamblin, 2004; Carpenter et al., 2017). For successful transmission, the virus must maintain its infectious properties within the insect's gut, a process that involves the removal of the outer capsid protein VP2, resulting in the formation of an infectious sub-viral particle (Marchi et al., 1995; Mertens et al., 1996; Darpel et al., 2011). This study provides the first evidence that AHSV VP7 functions as a viral attachment protein for insect cells. Despite the presence of an RGD motif in VP7, our findings suggest that this motif is not crucial for binding.

Our results challenge the hypothesis that the RGD motif in AHSV VP7 plays a functional role in binding insect cells. While the motif is situated

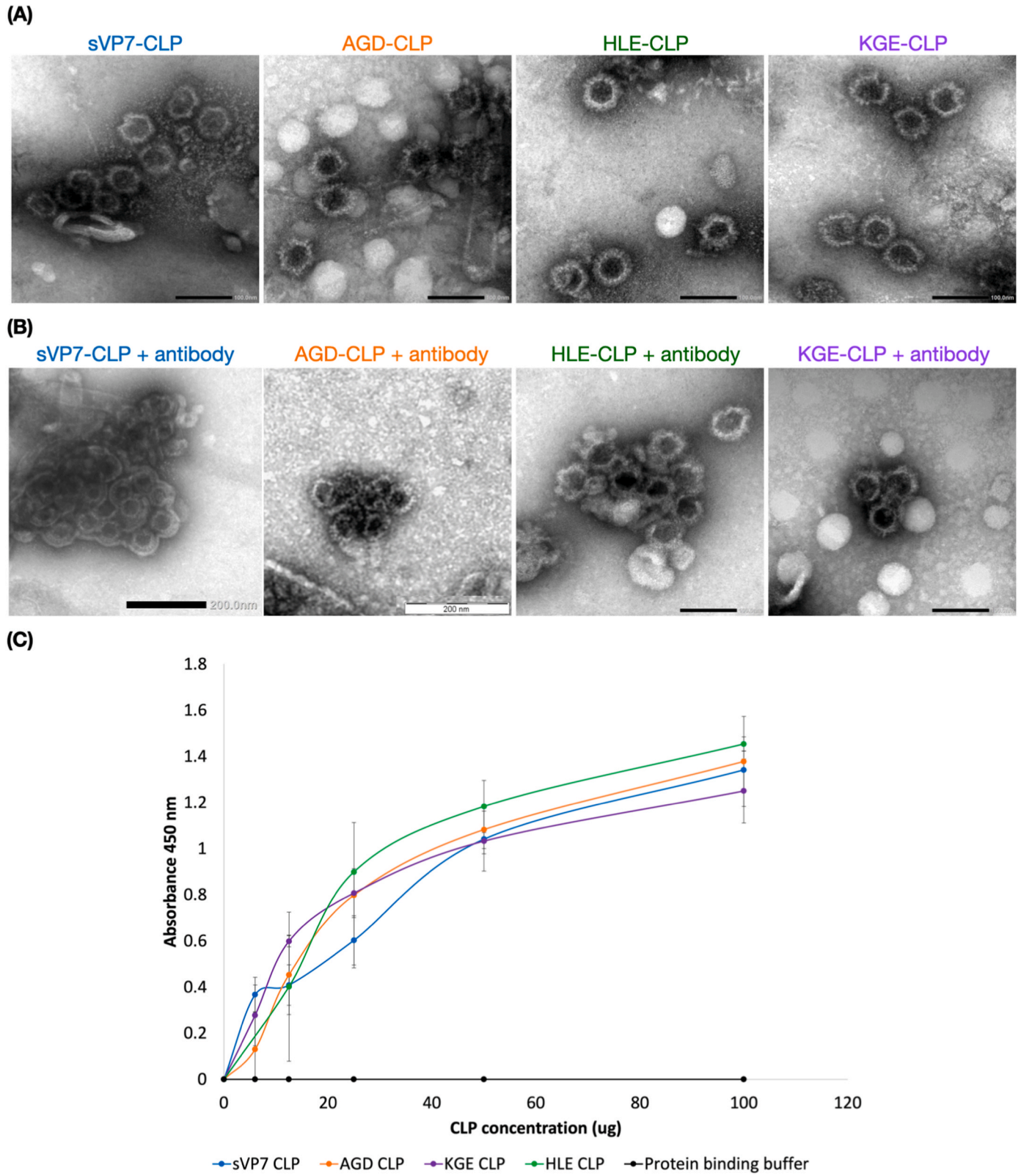

Fig. 2. Transmission electron micrographs and cell binding assay of the sVP7 and RGD-mutant CLPs. CLPs were obtained by co-expression of VP3 and either the sVP7 or a mutant sVP7 protein in Sf9 cells and purified through a discontinuous sucrose density gradient. The sVP7 CLP (indicated in blue), AGD CLP (indicated in orange), HLE CLP (indicated in green) and KGE CLP (indicated in purple) were incubated without (A) or with (B) an anti-VP7 polyclonal antibody and negatively stained with uranyl acetate prior to viewing of the samples by transmission electron microscopy. The size of the scale bar is 100–200 nm. (C) KC cell monolayers were incubated with an increasing concentration of the CLPs, and bound CLPs were detected with an ELISA using an anti-VP7 polyclonal antibody. The binding of CLPs is indicated as the absorbance at 450 nm and plotted against increasing CLP concentrations (0, 6, 12.5, 25, 50 or 100 μg/well). Protein binding buffer only was included as a negative control in the assay. The data represents the means ± SD of three independent experiments, with three technical repeats each. (For interpretation of the references to colour in this figure legend, the reader is referred to the Web version of this article.)

on an exposed loop and prior in silico docking studies suggested its involvement in binding to the I domain of integrins (Basak et al., 1996), we found that AHSV VP7 binds to KC cells independently of the RGD motif. This contrasts with a related arthropod-borne Orbivirus, BTV, where the RGD motif in VP7 is essential for cellular attachment to KC cells (Tan et al., 2001). The structural differences between the RGD motifs in AHSV and BTV may explain this disparity. In AHSV, the RGD motif is located in the lower part of the top domain, positioned deeper within the core on a less flexible loop comprising only 6 amino acids (residues 176–181), potentially limiting its accessibility for receptor interaction (Basak et al., 1996). Conversely, the BTV RGD motif is located at the upper part of the top domain at the surface of the core particle and resides on a more flexible loop consisting of 14 amino acids (Tan et al., 2001). This structural configuration of the BTV RGD motif is comparable to that of other non-enveloped viruses that bind to integrins, such as adenovirus and foot-and-mouth disease virus (FMDV), where it is also found on a longer loop (Lea et al., 1994). The observation that the RGD motif in AHSV VP7 is functionally silent parallels observations from other viruses such as coxsackievirus serotype 9 (CAV-9) (Hughes et al., 1995; Triantafilou et al., 2000) and a SAT2 type of FMDV, NAM/307/98 (Storey et al., 2007).

Currently, the interaction sites on the VP7 protein and specific cellular receptors that mediate AHSV VP7 interactions remain unidentified. However, these findings do not preclude the possibility that VP7 may interact with integrins present on the insect cell surface. While the importance of an RGD motif for integrin receptor binding is well-established, it has been demonstrated that integrins can also bind to non-RGD sequences, thereby facilitating viral binding and internalization (Graham et al., 2003; Stewart and Nemerow, 2007; Yang et al., 2021). Furthermore, the involvement of other cell surface molecules, such as carbohydrates, cellular proteins, and lipids, in mediating VP7 binding to the cell surface cannot be ruled out (Smith and Helenius, 2004; Yamauchi and Helenius, 2013). These attachment factors may function to concentrate virus particles on the host cell surface, preceding interaction with a specific cellular receptor (Grove and Marsh, 2011; Casasnovas, 2013).

5. Conclusion

This study enhances our understanding of the initial stages of AHSV infection in its insect vector by revealing that AHSV VP7 binds to insect cells independently of the RGD motif. This finding is particularly notable given that in a related orbivirus, BTV, the RGD motif in VP7 is essential for cellular attachment to KC cells (Tan et al., 2001). Given that the outer capsid protein VP2 of AHSV facilitates the binding and infection of mammalian cells (Hassan and Roy, 1999; Wu and Roy, 2022), the observed role of VP7 in insect cell binding implies the potential engagement of alternative cellular receptors and internalization pathways in the vector insect compared to the vertebrate host. Further research is required to identify not only the interaction sites on the VP7 protein, but also the specific cellular receptors and internalization pathways involved in insect cell infection. This will be crucial for enhancing our understanding of AHSV-host interactions in the *Culicoides* vector.

CRediT authorship contribution statement

Ariel Renée Monique Buyens: Writing – original draft, Visualization, Methodology, Investigation, Formal analysis, Data curation. **Vida van Staden:** Writing – review & editing, Supervision, Resources, Formal analysis. **Jacques Theron:** Writing – review & editing, Supervision, Resources, Project administration, Funding acquisition, Formal analysis, Conceptualization.

Ethics statement

Ethical approval was not required for this research.

Funding

This work was funded by the Poliomyelitis Research Foundation (Grant 18/89).

Declaration of competing interest

The authors declare that they have no known competing financial interests or personal relationships that could have appeared to influence the work reported in this paper.

Acknowledgements

The authors would like to acknowledge the technicians at the Laboratory for Microscopy and Microanalysis at the University of Pretoria, South Africa, for the use of their equipment. Erna van Wilpe and Charity Maepa at the Hatfield campus, and Dr Antoinette Lensink at the Onderstepoort campus. The authors thank Professor Michael S. Pepper for granting permission to use BioRender Premium to create the graphical abstract.

Appendix A. Supplementary data

Supplementary data to this article can be found online at https://doi.org/10.1016/j.virol.2025.110694.

Data availability

Data will be made available on request.

References

Basak, A.K., Gouet, P., Grimes, J., Roy, P., Stuart, D., 1996. Crystal structure of the top domain of AHSV VP7: comparisons with BTV VP7. J. Virol. 70, 3797–3806.
Bekker, S.M., Burger, P., van Staden, V., 2017. Analysis of the three-dimensional structure of the African horse sickness virus VP7 trimer by homology modelling. Virus Res. 232, 80–95.
Bekker, S.M., Huismans, H., van Staden, V., 2014. Factors that affect the intracellular localization and trafficking of AHSV core protein, VP7. Virol. J. 456, 279–291.
Bekker, S.M., Huismans, H., van Staden, V., 2022a. Generation of a soluble African horse sickness virus VP7 protein capable of forming core-like particles. Viruses 14, 1624.
Bekker, S.M., Potgieter, C.A., van Staden, V., Theron, J., 2022b. Investigating the role of African horse sickness virus VP7 protein crystalline particles on virus replication and release. Viruses 14, 2193.
Blancher, C., Jones, A., 2001. SDS-PAGE and western blotting techniques. In: *Metastasis Research Protocols: Volume I: Analysis of Cells and Tissues*. Humana Press, Totowa, NJ, pp. 145–162.
Burroughs, J., O'Hara, R., Smale, C., Hamblin, C., Walton, A., Armstrong, R., Mertens, P., 1994. Purification and properties of virus particles, infectious subviral particles, cores and VP7 crystals of African horse sickness virus serotype 9. J. Gen. Virol. 75, 1849–1857.
Carpenter, S., Mellor, P., Fall, A., Garros, C., Venter, G., 2017. African horse sickness virus: history, transmission, and current status. Annu. Rev. Entomol. 62, 343–358.
Casasnovas, J.M., 2013. Virus - receptor interactions and receptor-mediated virus entry into host cells. Subcell. Biochem. 64, 441–466.
Darpel, K.E., Langner, K.F.A., Nimtz, M., Anthony, S.J., Brownlie, J., Takamatsu, H.H., Mellor, P.S., Mertens, P.P.C., 2011. Saliva proteins of vector *Culicoides* modify structure and infectivity of bluetongue virus particles. PLoS One 6, e17545.
French, T.J., Roy, P., 1990. Synthesis of BTV core-like particles by a recombinant baculovirus expressing the two major structural core proteins of BTV. J. Virol. 64, 1530–1536.
Graham, K.L., Halasz, P., Tan, Y., Hewish, M.J., Takada, Y., Mackow, E.R., Robinson, M. K., Coulson, B.S., 2003. Integrin-using rotaviruses bind α2β1 integrin α2 I domain via VP4 DGE sequence and recognize αXβ2 and αVβ3 by using VP7 during cell entry. J. Virol. 77, 9969–9978.
Grove, J., Marsh, M., 2011. The cell biology of receptor-mediated virus entry. J. Cell Biol. 195, 1071–1082.
Gulati, N.M., Torian, U., Gallagher, J.R., Harris, A.K., 2019. Immunoelectron microscopy of viral antigens. Curr. Protoc. Microbiol. 53, e86.
Hassan, S., Roy, P., 1999. Expression and characterization of bluetongue virus VP2 protein: role in cell entry. J. Virol. 73, 9832–9842.

Hughes, P.J., Horsnell, C., Hyypiä, T., Stanway, G., 1995. The coxsackievirus A9 RGD motif is not essential for virus viability. J. Virol. 69, 8035–8040.
King, S., Rajko-Nenow, P., Ashby, M., Frost, L., Carpenter, S., Batten, C., 2020. Outbreak of African horse sickness in Thailand. Transbound. Emerg. Dis. 67, 1764–1767.
Laemmli, U.K., 1970. Cleavage of structural proteins during the assembly of the head of bacteriophage T4. Nature 227, 680–685.
Lea, S., Hernandez, J., Blakemore, W., Brocchi, E., Curry, S., 1994. The structure and antigenicity of a type C foot-and-mouth disease virus. Structure 2, 123–139.
Limn, C., Staeuber, N., Monastyrskaya, K., Gouet, P., Roy, P., 2000. Functional dissection of the major structural protein of bluetongue virus - identification of key residues within VP7 essential for capsid assembly. J. Virol. 74, 8658–8669.
Manole, V., Laurinmäki, P., van Wyngaardt, W., Potgieter, A.C., Wright, I.M., 2012. Structural insight into African horse sickness virus infection. J. Virol. 86, 7858–7866.
Marchi, P.R., Rawlings, P., Burroughs, J.N., Wellby, M., 1995. Proteolytic cleavage of VP2, an outer capsid protein of African horse sickness virus, by species-specific serum proteases enhances infectivity in *Culicoides*. J. Gen. Virol. 76, 2607–2611.
Maree, S., Maree, F.F., Putterill, J.F., de Beer, T.A.P., Huismans, H., Theron, J., 2016. Synthesis of empty AHS particles. Virus Res. 213, 184–194.
Mellor, P.S., Hamblin, C., 2004. African horse sickness. Vet. Res. 35, 445–466.
Mertens, P., Burroughs, J.N., Walton, A., Wellby, M.P., 1996. Enhanced infectivity of modified BTV particles for two insect cell lines and for two *Culicoides* vector species. Virol. J. 217, 582–593.
Monastyrskaya, K., Staeuber, N., Sutton, G., Roy, P., 1997. Effects of domain-switching and site-directed mutagenesis on the properties and functions of the VP7 proteins of two orbiviruses. Virol. J. 237, 217–227.
Patel, A., Roy, P., 2014. The molecular biology of bluetongue virus replication. Virus Res. 182, 5–20.
Smith, A.E., Helenius, A., 2004. How viruses enter cells. Science 304, 237–242.
Stewart, P.L., Nemerow, G.R., 2007. Cell integrins: commonly used receptors for diverse viral pathogens. Trends Microbiol. 15, 500–507.
Storey, P., Theron, J., Maree, F.F., O'Neill, H.G., 2007. A second RGD motif in the 1D capsid protein of a SAT1 type foot-and-mouth disease virus field isolate is not essential for attachment to target cells. Virus Res. 124, 184–192.
Tan, B.H., Nason, E., Staeuber, N., Jiang, W., 2001. RGD tripeptide of bluetongue virus VP7 protein is responsible for core attachment to *Culicoides* cells. J. Virol. 75, 3937–3947.
Triantafilou, M., Triantafilou, K., Wilson, K.M., Takada, Y., Fernandez, N., 2000. High affinity interactions of Coxsackievirus A9 with integrin αvβ3 (CD51/61) require the CYDMKTTC sequence of β3, but do not require the RGD sequence of the CAV-9 VP1 protein. Hum. Immunol. 61, 453–459.
Wu, W., Roy, P., 2022. Sialic acid binding sites in VP2 of bluetongue virus and their use during virus entry. J. Virol. 96, e0167721.
Xu, G., Wilson, W., Mecham, J., Murphy, K., 1997. VP7: an attachment protein of BTV for cellular receptors in *Culicoides variipennis*. J. Gen. Virol. 78, 1617–1623.
Yamauchi, Y., Helenius, A., 2013. Virus entry at a glance. J. Cell Sci. 126, 1289–1295.
Yang, J., Park, J., Koehler, M., Simpson, J., Luque, D., Rodríguez, J.M., Alsteens, D., 2021. Rotavirus binding to cell surface receptors directly recruiting α2 integrin. Adv. Nanobiomed Res. 1, 2100077.
Zientara, S., Weyer, C.T., Lecollinet, S., 2015. African horse sickness. Rev. Sci. Tech. 34, 315–327.